Rheology of a Combined Main-Chain/Side-Chain Liquid-Crystalline Polymer in the Thermotropic and Lyotropic States

Ming Zhou and Chang Dae Han*

Department of Polymer Engineering, The University of Akron, Akron, Ohio 44325

Received March 29, 2005; Revised Manuscript Received October 24, 2005

ABSTRACT: The rheological behavior of a combined main-chain/side-chain liquid-crystalline polymer, PSHQ4−7CNCOOH, has been investigated in both the thermotropic and lyotropic states. The synthesis procedures for PSHQ4−7CNCOOH are described in a previous paper. In this study transient shear flow, steady-state shear flow, oscillatory shear flow, and time evolution of dynamic moduli upon cessation of shear flow of PSHQ4−7CNCOOH in the thermotropic state have been investigated. Only positive values of first normal stress difference (N_1) in steady-state shear flow were observed over the entire range of shear rates and temperatures investigated. One of the objectives of this study was to investigate the role of the side-chain mesogenic groups (7CNCOOH), which were grafted onto the flexible methylene units of the main-chain backbone (PSHQ4), in influencing the rheological behavior of PSHQ4−7CNCOOH in the thermotropic state. Thus, for comparison, the rheological behavior of PSHQ4 was also investigated. Another objective of this study was to investigate the rheological behavior of PSHQ4−7CNCOOH in the lyotropic state. For this, lyotropic solutions of various concentrations (22−70 wt %) of PSHQ4−7CNCOOH dissolved in *o*-dichlorobenzene were prepared for rheological measurements. The major thrust was to investigate whether the lyotropic solutions of PSHQ4−7CNCOOH might give rise to negative values of N_1 in steady-state shear flow. Indeed, negative values of N_1 were observed at intermediate shear rates for lyotropic solutions of PSHQ4−7CNCOOH having concentrations up to ca. 27 wt %. Interestingly, negative values of N_1 became positive as the measurement temperature decreased below a certain critical value. Thus, the sign of N_1 is found to depend on both the concentration and temperature of the lyotropic solutions of PSHQ4−7CNCOOH. Also, flow reversal of lyotropic solutions of PSHQ4−7CNCOOH was investigated. It has been found that both shear stress and first normal stress difference do not follow strain scaling after flow reversal. The experimental results of this study are discussed in the context of currently held theories.

1. Introduction

During the past three decades numerous research groups have conducted experimental investigations on the rheological behavior of liquid-crystalline polymers (LCP). Some investigators reported on the rheological behavior of lyotropic solutions of poly(γ-benzyl L-glutamate) (PBLG),[1−14] hydroxypropylcellulose (HPC),[15−21] and other rodlike stiff polymers,[22−27] while other investigators reported on the rheological behavior of thermotropic main-chain LCPs[28−42] and still others reported on the rheological behavior of thermotropic side-chain LCPs.[43−56]

One of the unresolved issues today in experimental LCP rheology is the sign of first normal stress difference (N_1) in steady-state shear flow. Specifically, since the seminal papers by Kiss and Porter,[2−4] who first reported *negative* values of N_1 in steady-state shear flow over a certain range of shear rates for lyotropic solutions of PBLG, other investigators[16−18,21] have reported similar experimental observations for lyotropic solutions of HPC. The origin of such unusual rheological behavior of some lyotropic solutions was explained theoretically by Marrucci and Maffettone[57] and Larson.[58] According to Marrucci and Maffettone,[57] the occurrence of a negative N_1 is associated with a flow transition between director tumbling and flow-aligning behavior. Larson[58] coined the term "wagging" to describe the region representing the transition from the tumbling to the nontumbling flow (flow-aligning) regime. On the other hand, so far only *positive* values of N_1 have been reported over the entire range of shear rates tested for thermotropic LCPs.[31−36,38−42]

One practical approach to resolve the issue at hand is to employ an LCP that exhibits both thermotropic and lyotropic characteristics. To this end, earlier, Baek et al.[18] employed HPC to investigate its rheological behavior in both the lyotropic and thermotropic states. They observed that values of N_1 for lyotropic solutions of HPC were negative below a certain critical concentration and then became positive at higher concentrations. They offered plausible interpretations of their experimental results. To our knowledge, however, no investigation has ever been reported on the rheological behavior of a synthetic LCP in both the thermotropic and lyotropic states. The paucity of the literature reporting on the rheological behavior of a synthetic LCP in both lyotropic and thermotropic states is due to the unavailability of an LCP that exhibits both thermotropic and lyotropic characteristics. For such purposes, an LCP must have (i) a sufficiently low clearing temperature that lies below the thermal degradation temperature and (ii) a nematic mesophase in the thermotropic state that enables one to obtain rheological measurements. Note that a thermotropic main-chain LCP having a smectic mesophase is not suitable for rheological measurements because it is too viscous to flow. Therefore, an ideal LCP must be sufficiently bulky in chemical structure, prohibiting the formation of a closely packed state and thus giving rise to a glassy state, such that it would not crystallize or precipitate out when it is dissolved in a suitable solvent. The synthesis of such an LCP requires a well-thought-out molecular design because most of the thermotropic LCPs synthesized to date first crystallize or precipitate out when they are dissolved in a solvent, prohibiting the formation of lyotropic solutions.

In our very recent study,[59] we have reported the synthesis of a combined main-chain/side-chain liquid-crystalline polymer, referred to as PSHQ4−7CNCOOH, with the chemical structure

* To whom correspondence should be addressed. E-mail: cdhan@uakron.edu.

10.1021/ma050657a CCC: $33.50
Published on Web 11/23/2005

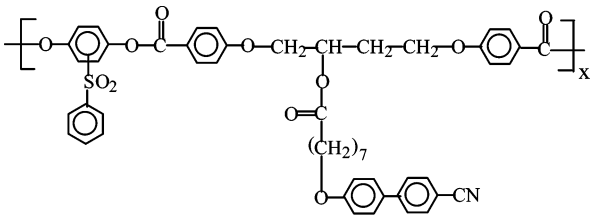

PSHQ4−7CNCOOH

which meets all the requirements delineated above for the preparation of lyotropic solutions. Specifically, PSHQ4−7CNCOOH has a glass transition temperature (T_g) of 85 °C and a nematic-to-isotropic (N−I) transition temperature (T_{NI}) of 172 °C, while it begins to undergo thermal degradation at ca. 350 °C. Moreover, PSHQ4−7CNCOOH is a glassy polymer. In general, it is very difficult to prepare lyotropic solutions from a thermotropic LCP; however, we have successfully prepared lyotropic solutions over a very wide range of concentrations (22−70 wt %) from PSHQ4−7CNCOOH.[59] Thus, we thought that PSHQ4−7CNCOOH was an ideal LCP that would enable us to investigate its rheological behavior in both the thermotropic and lyotropic states.

Indeed, we have investigated the rheological behavior of PSHQ4−7CNCOOH in both the thermotropic and lyotropic states over a very wide range of concentrations, shear rates, and temperatures. We have observed negative values of N_1 at an intermediate range of shear rates for concentrations up to 27 wt % and only positive values of N_1 for higher concentrations including the thermotropic state over the entire range of shear rates investigated. Interestingly, we have observed that negative values of N_1 for low concentrations (22, 25, and 27 wt %) of lyotropic solutions of PSHQ4−7CNCOOH became positive as the measurement temperature decreased below a certain critical value. Thus, we have concluded that both the temperature and concentration of lyotropic solutions play a decisive role in determining the sign of N_1 of lyotropic solutions of PSHQ4−7CNCOOH. To our knowledge, no such investigation has ever been reported in the literature that employed a synthetic LCP. In this paper we summarize the highlights of our findings.

2. Experimental Section

Materials. In the present study we employed PSHQ4−7CNCOOH that was synthesized in our recent study.[59] The details of the synthesis procedures for PSHQ4−7CNCOOH are described in our previous paper.[59] We have confirmed the chemical structure of PSHQ4−7CNCOOH using proton and carbon-13 nuclear magnetic resonance spectroscopy and Fourier transform infrared spectroscopy. Further, (i) using differential scanning calorimetry (DSC), we have determined that PSHQ4−7CNCOOH has a glass transition temperature (T_g) of 85 °C and T_{NI} of 172 °C; (ii) using polarized optical microscopy (POM), we have determined that PSHQ4−7CNCOOH has only nematic structure over the entire range of temperatures between T_g and T_{NI}; (iii) using wide-angle X-ray diffraction (WAXD), we have concluded that PSHQ4−7CNCOOH is a glassy polymer. For comparison purposes, we also investigated the rheological behavior of a main-chain LCP, PSHQ4, with the chemical structure

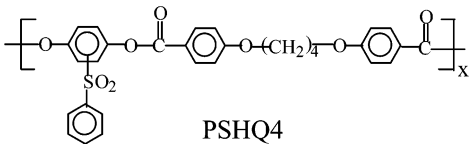

PSHQ4

which is exactly the same as the main-chain backbone of PSHQ4−7CNCOOH. We have not been able to prepare lyotropic solutions from PSHQ4. This is because being a well-ordered semicrystalline polymer, PSHQ4 precipitates out with crystals as the solvent evaporates. In our previous paper,[59] we compared the thermal transition temperatures and mesophase structure of PSHQ4 with those of PSHQ4−7CNCOOH.

Preparation of Bulk PSHQ4−7CNCOOH Specimens for Rheological Measurement. We prepared bulk PSHQ4−7CNCOOH specimens by dissolving a predetermined amount of polymer in dichloromethane, followed by a slow evaporation of the solvent initially and then complete removal of solvent in a vacuum oven. Drying continued until no change in weight was observed, and the dried specimens were kept in a refrigerator until use.

Preparation of Lyotropic Solutions of PSHQ4−7CNCOOH for Rheological Measurement. We prepared lyotropic solutions of PSHQ4−7CNCOOH using the procedures described in our previous paper.[59] We found that PSHQ4−7CNCOOH dissolves in *o*-dichlorobenzene, *m*-dibromobenzene, and tetrachloroethane. For the rheological investigation reported here we employed lyotropic solutions of PSHQ4−7CNCOOH dissolved in *o*-dichlorobenzene, having the following concentrations: 22, 25, 27, 30, 37, 40, 50, 60, and 70 wt %. Note that the boiling point of *o*-dichlorobenzene is above 180 °C, which then enabled us to conduct rheological measurements between 0 and 60 °C with little loss of solvent. The solutions thus prepared were stored at low temperature until use for rheological measurements.

Rheological Measurement. In the present study, an Advanced Rheometrics Expansion System (ARES, TA Instruments) was employed for rheological investigation. For the rheological measurements of PSHQ4−7CNCOOH in the thermotropic state, we employed an 8 mm cone-and-plate fixture for transient and steady-state shear flow measurements and an 8 mm parallel-plate fixture for oscillatory shear flow measurements. For the rheological measurements of lyotropic solutions of PSHQ4−7CNCOOH, we employed a 50 mm cone-and-plate fixture for transient and steady-state shear flow measurements. In the rheological measurements of PSHQ4−7CNCOOH in the thermotropic state, a specimen was placed in a cone-and-plate fixture or parallel-plate fixture that had been heated to ca. 190 °C, about 18 °C above the T_{NI} of PSHQ4−7CNCOOH, and sheared at a shear rate of 0.1 s^{-1} for 10 min in order to erase any previous thermal history. Then the specimen was cooled very slowly to a predetermined temperature in the nematic state. Before measurement began, we waited for a sufficiently long time until the normal force was stabilized at a baseline. For transient shear flow experiments, the growth of first normal stress difference ($N_1^+(\dot\gamma,t)$) and the growth of shear stress ($\sigma^+(\dot\gamma,t)$) were recorded until reaching steady state at predetermined temperature and shear rate ($\dot\gamma$). For oscillatory shear flow measurements, dynamic storage modulus (G') and dynamic loss modulus (G'') were recorded as functions of angular frequency (ω) and temperature. Using G' and G'', the absolute values of complex viscosity $|\eta^*(\omega)|$ were calculated with the relationship $|\eta^*(\omega)| = [(G'(\omega)/\omega)^2 + (G''(\omega)/\omega)^2]^{0.5}$. Strain amplitude was varied from 0.01 to 0.06, which was well within the linear viscoelasticity range of the materials investigated. Also, the time evolution of dynamic moduli (G' and G'') upon cessation of steady-state shear flow at $\dot\gamma = 1.0$ s^{-1} was investigated at various temperatures for PSHQ4−7CNCOOH. All experiments were conducted under a nitrogen atmosphere in order to preclude oxidative degradation of the specimen. The temperature control was satisfactory to within ±1 °C.

3. Results

3.1. Rheological Behavior of PSHQ4−7CNCOOH in the Thermotropic State. Figure 1 gives (a) plots of shear stress buildup $\sigma^+(\dot\gamma,t)$ vs strain $\dot\gamma t$ and (b) plots of first normal stress difference buildup $N_1^+(\dot\gamma,t)$ vs $\dot\gamma t$ upon startup of shear flow of PSHQ4−7CNCOOH at 130 °C for five different shear rates. It can be seen in Figure 1 that $\sigma^+(\dot\gamma,t)$ exhibits an overshoot, the

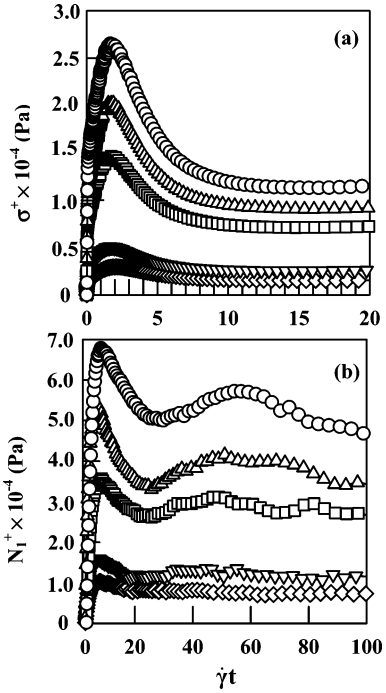

Figure 1. Plots of (a) $\sigma^+(\dot{\gamma},t)$ vs $\dot{\gamma}t$ and (b) $N_1^+(\dot{\gamma},t)$ vs $\dot{\gamma}t$ during transient shear flow of PSHQ4−7CNCOOH at 130 °C at different shear rates (s^{-1}): (○) 1.5, (△) 1.0, (□) 0.6, (▽) 0.3, and (◇) 0.1.

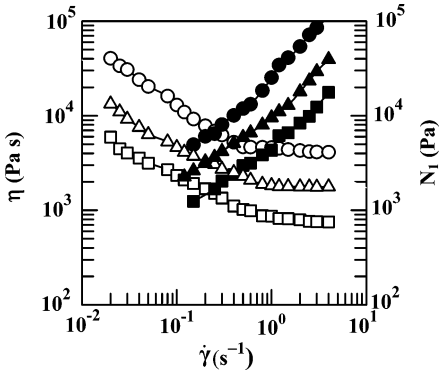

Figure 2. Plots of log η vs log $\dot{\gamma}$ (open symbols) and log N_1 vs log $\dot{\gamma}$ (filled symbols) in steady-state shear flow of PSHQ4−7CNCOOH at different temperatures (°C): (○, ●) 130, (△, ▲) 140, and (□, ■) 150.

magnitude of which increases with increasing shear rate and reaches steady state for $\dot{\gamma}t$ less than 10. The behavior of $N_1^+(\dot{\gamma},t)$ at $\dot{\gamma} \geq 0.6$ s^{-1} shows an oscillatory decay with a second overshoot before reaching steady state, while $N_1^+(\dot{\gamma},t)$ for $\dot{\gamma} \leq 0.3$ s^{-1} shows a small overshoot and reaches steady state rather quickly. A very similar observation was made for the main-chain LCP, PSHQ4, the results of which are given in the Supporting Information. That is, grafting of side-chain mesogenic group 7CNCOOH onto the flexible spacer of PSHQ4 has little influence on the transient shear flow behavior of PSHQ4−7CNCOOH.

Figure 2 gives logarithmic plots of shear viscosity η vs shear rate $\dot{\gamma}$ (open symbols) and logarithmic plots of first normal stress difference N_1 vs $\dot{\gamma}$ (filled symbols) in steady-state shear flow of PSHQ4−7CNCOOH at three different temperatures. It is seen in Figure 2 that PSHQ4−7CNCOOH shows shear-thinning behavior (so-called region I) at low values of shear rates ($\dot{\gamma}$ < ca. 1 s^{-1}) followed by Newtonian behavior (so-called region II) at higher shear rates ($\dot{\gamma}$ > ca. 1 s^{-1}). One can infer from Figure 2 that at $\dot{\gamma}$ > ca. 1 s^{-1} the magnitude of N_1 is larger than that of shear stress (σ). Of particular note in Figure 2 is

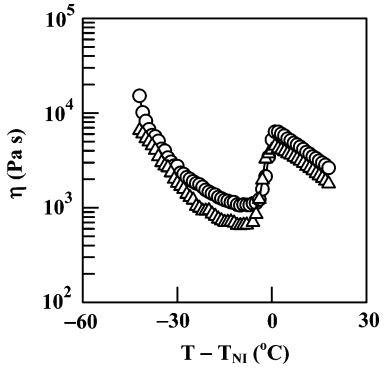

Figure 3. Variations of η with $T - T_{NI}$ for PSHQ4−7CNCOOH during steady-state temperature sweep experiments at two different shear rates (s^{-1}): (○) 0.1 and (△) 1.0, where T_{NI} denotes N−I transition temperature of PSHQ4−7CNCOOH.

that the sign of N_1 is positive over the entire range of shear rates and temperatures investigated. We have found that the main-chain LCP, PSHQ4, has similar shear-rate dependence of η and N_1, the results of which are given in the Supporting Information, indicating that grafting of side-chain mesogenic group 7CNCOOH onto the flexible spacer of PSHQ4 has little influence on the shear-rate dependence of η and N_1 for PSHQ4−7CNCOOH.

Figure 3 describes the temperature dependence of η for PSHQ4−7CNCOOH obtained during temperature sweep experiments at two different shear rates, 0.1 and 1.0 s^{-1}, where T_{NI} denotes N−I transition temperature of PSHQ4−7CNCOOH. It is of interest to observe in Figure 3 that η initially decreases rapidly with increasing temperature and then begins to increase before reaching T_{NI}, going through a maximum at T_{NI}, and then decreases again with a further increase in temperature. An increase in η as the temperature approaches the T_{NI} of PSHQ4−7CNCOOH is due to the loss of liquid crystallinity in PSHQ4−7CNCOOH as the anisotropic polymer is becoming an isotropic fluid. Note that the viscosity of an LCP in the anisotropic region, owing to the orientation of LCP during shear flow, is expected to be lower than that in the isotropic region. We made a similar observation of the temperature dependence of η during temperature sweep experiments of PSHQ4, the results of which are given in the Supporting Information. We thus conclude that grafting of side-chain mesogenic group 7CNCOOH onto the flexible spacer of PSHQ4 has little influence on the temperature dependence of η for PSHQ4−7CNCOOH.

Figure 4 compares the frequency dependence of complex viscosity $|\eta^*|$ for PSHQ4−7CNCOOH with that for PSHQ4 at seven different temperatures. It is not possible to prepare log $|\eta^*|$ vs log ω plots for the two LCPs at the same temperatures because the T_{NI} (260 °C) of PSHQ4 is much higher than that (170 °C) of PSHQ4−7CNCOOH. It can be seen in Figure 4 that at temperatures below the respective T_{NI}s the frequency dependence of $|\eta^*|$ looks somewhat similar in both PSHQ4−7CNCOOH and PSHQ4, although PSHQ4−7CNCOOH shows shear-thinning behavior over the entire range of frequencies investigated. What is of great interest in Figure 4 is the difference in frequency dependence of $|\eta^*|$ between PSHQ4−7CNCOOH and PSHQ4 at temperatures above the respective T_{NI}s. Specifically, for ω < 1 rad/s, the $|\eta^*|$ of PSHQ4 follows Newtonian behavior, while the $|\eta^*|$ of PSHQ4−7CNCOOH does not. The physical origin of the observed difference between the two polymers is not clear.

Figure 5 describes the time evolution of dynamic storage modulus G' upon cessation of steady-state shear flow at $\dot{\gamma}$ =

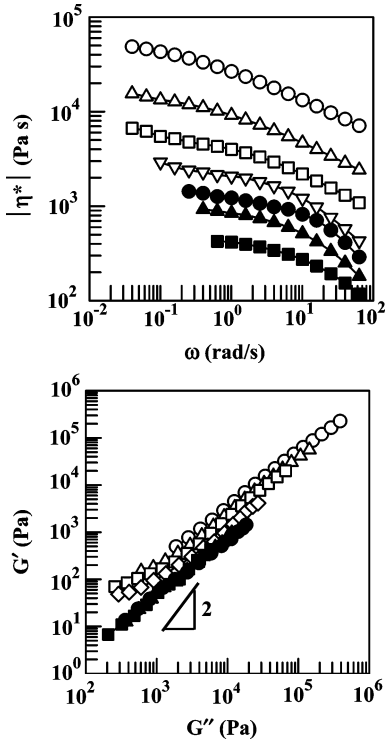

Figure 4. Plots of log $|\eta^*|$ vs log ω for (a) PSHQ4−7CNCOOH at various temperatures (°C): (○) 130, (△) 140, (□) 150, (▽) 160, (●) 175, (▲) 180, and (■) 185, and (b) PSHQ4 at various temperatures (°C): (○) 220, (△) 230, (□) 240, (▽) 250, (●) 260, (▲) 265, and (■) 270.

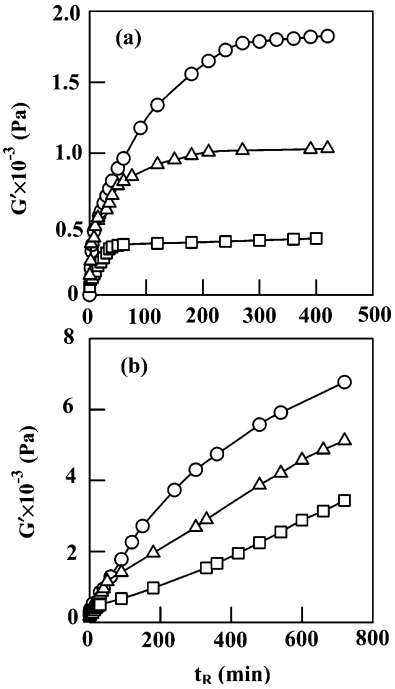

Figure 5. Time evolution of dynamic storage modulus G' upon cessation of steady-state shear flow at $\dot{\gamma} = 1.0\ s^{-1}$, which was monitored at an angular frequency of 1.0 rad/s for (a) PSHQ4−7CNCOOH at different temperatures (°C): (○) 130, (△) 140, and (□) 150; (b) PSHQ4 at different temperatures (°C): (○) 220, (△) 230, and (□) 240.

1.0 s^{-1}, which was monitored at an angular frequency of 1.0 rad/s for (a) PSHQ4−7CNCOOH at 130, 140, and 150 °C and (b) PSHQ4 at 220, 230, and 240 °C. Note that the measurement temperatures for each polymer were chosen, such that they have the same distance from the T_{NI} of the respective polymers (T_{NI} = 170 °C for PSHQ4−7CNCOOH and T_{NI} = 260 °C for PSHQ4). For instance, the measurement temperature 130 °C for PSHQ4−7CNCOOH and the measurement temperature 220 °C for PSHQ4 are at the same distance from the respective T_{NI}s. Previously, such an approach was successfully employed to compare the viscosities of main-chain LCPs having different flexible spacers and thus different molecular weights.[39] The rationale behind the approach lies in that since T_{NI} reflects the chemical structures of polymers and, also, depends on their molecular weights,[34] comparison of the rheological behavior of the two polymers at $T - T_{NI}$ can be regarded as being independent of their molecular weights. The following observations are worth noting in Figure 5. Upon cessation of shear flow at 1.0 s^{-1}, the G' of PSHQ4−7CNCOOH initially increases very fast and then levels off, reaching a constant value after ca. 50 min at 150 °C, after ca. 200 min at 140 °C, and after ca. 350 min at 130 °C. The magnitude of G' for PSHQ4−7CNCOOH increases as the temperature is decreased. On the other hand, the G' of PSHQ4 does not attain a constant value even after 750 min upon cessation of shear flow at 1.0 s^{-1}. An increase in G' upon cessation of shear flow may be viewed as signifying a recovery of the deformed domain structure (i.e., structural reorganization) after shear flow stops. We can then conclude from Figure 5 that upon cessation of shear flow a faster structural reorganization takes place in PSHQ4−7CNCOOH than in PSHQ4.

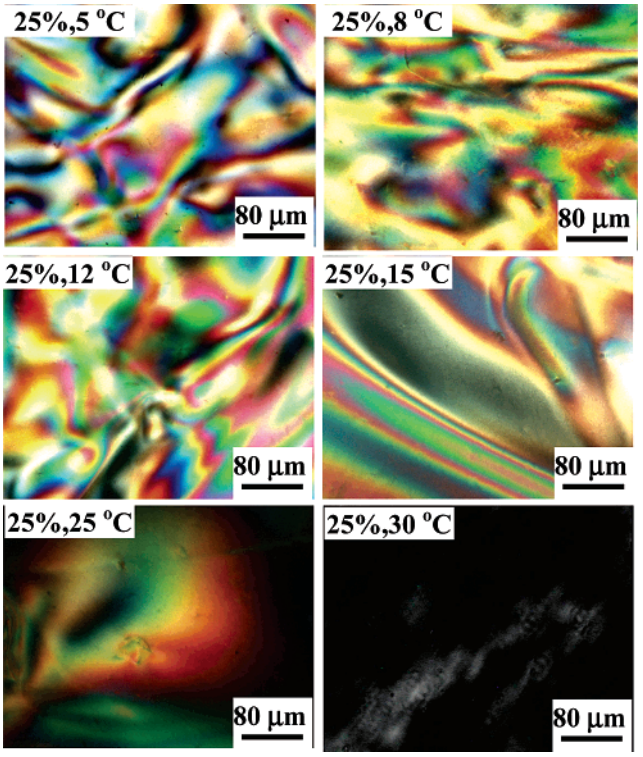

Figure 6. POM images of 25 wt % lyotropic solution of PSHQ4−7CNCOOH in *o*-dichlorobenzene at various temperatures as indicated on each image.

3.2. Rheological Behavior of Lyotropic Solutions of PSHQ4−7CNCOOH. (a) Phase Behavior of Lyotropic Solutions of PSHQ4−7CNCOOH. Polarized optical microscopy (POM) images at various temperatures are given in Figure 6 for 25 wt % lyotropic solution of PSHQ4−7CNCOOH dissolved in *o*-dichlorobenzene. The POM images were also obtained for the lyotropic solutions having other concentrations (22, 27, 30, 37, 40, 45, 60, and 70 wt %). It is seen from Figure 6 that 25 wt % solution has become isotropic (the dark image) at 30 °C. In our previous paper,[59] we presented a phase diagram for the

Table 1. Clearing Temperatures of Lyotropic Solutions of PSHQ4−7CNCOOH As Determined by Polarizing Optical Microscopy

concn (wt %)	22	25	27	30	37	40	50	60
T_{cl} (°C)	10	15	20	28	39	43	63	81

lyotropic solutions with concentrations varying from 22 to 70 wt % of PSHQ4−7CNCOOH in three different solvents. In the phase diagram we observed a narrow biphasic region between the isotropic and nematic regions. In the present study, we took rheological measurements of several lyotropic solutions (22, 25, 27, 30, 37, 40, 50, and 60 wt %) at temperatures below the clearing temperature (T_{cl}) of each lyotropic solution. To facilitate our discussion below when presenting the results of our rheological measurements, Table 1 gives a list of T_{cl} for the solutions employed.

(b) Transient Shear Flow Behavior of Lyotropic Solutions of PSHQ4−7CNCOOH. Figure 7 describes the time evolution of first normal stress difference $N_1^+(\dot{\gamma},t)$ and shear stress $\sigma^+(\dot{\gamma},t)$ at $\dot{\gamma} = 0.08\ s^{-1}$ for 25 wt % lyotropic solution of PSHQ4−7CNCOOH at 12, 8, and 5 °C. Note that the T_{cl} of the solution is 15 °C (see Table 1). The following observations are worth noting in Figure 7. (i) At 12 °C, $N_1^+(\dot{\gamma},t)$ shows a large overshoot followed by a small overshoot, and then it decays to a constant value with negative sign. (ii) When the temperature is decreased to 8 °C, $N_1^+(\dot{\gamma},t)$ shows a large overshoot and then quickly decays to a constant value with positive sign. (iii) When the temperature is decreased further to 5 °C, $N_1^+(\dot{\gamma},t)$ again goes through an overshoot followed by rapid decay to a constant value with positive sign. (iv) At all three temperatures investigated, $\sigma^+(\dot{\gamma},t)$ goes through a single overshoot followed by rapid decay to a constant value with positive sign. Both the magnitude of the overshoot and the value of steady-state shear stress (σ) increase as the temperature is decreased from 12 to 5 °C.

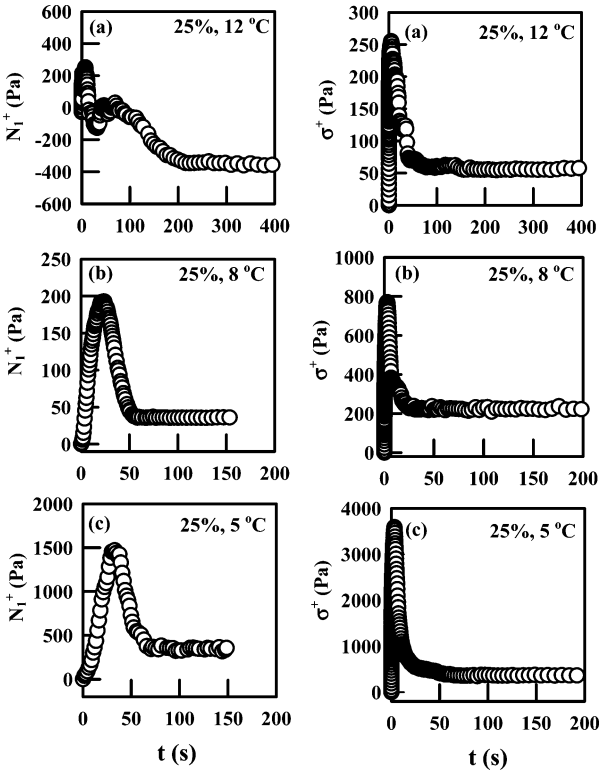

Figure 7. Left-side panel describes time evolution, upon start-up of shear, of first normal stress difference $N_1^+(\dot{\gamma},t)$ and the right-side panel describes time evolution, upon start-up of shear, of shear stress $\sigma^+(\dot{\gamma},t)$ for 25 wt % lyotropic solution of PSHQ4−7CNCOOH in *o*-dichlorobenzene at $\dot{\gamma} = 0.08\ s^{-1}$ and three different temperatures (°C): 12, 8, and 5.

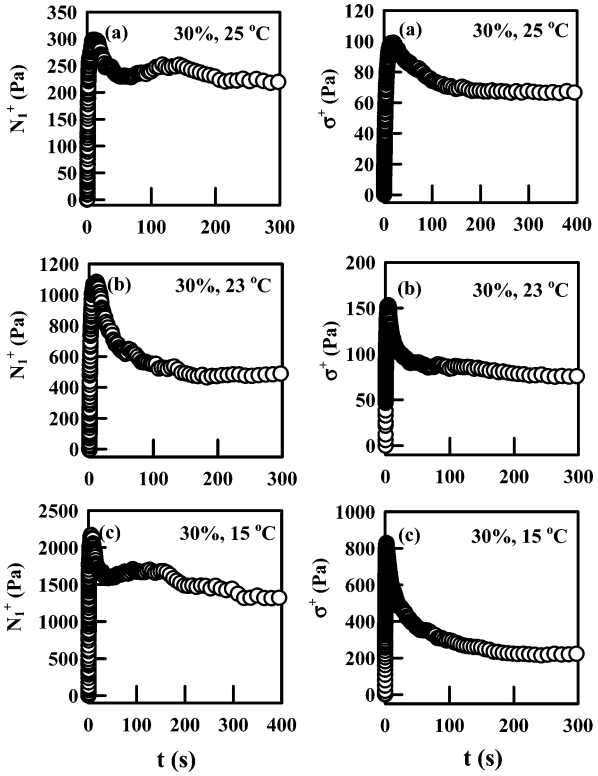

Figure 8. The left-side panel describes time evolution, upon start-up of shear, of first normal stress difference $N_1^+(\dot{\gamma},t)$ and the right-side panel describes time evolution, upon start-up of shear, of shear stress $\sigma^+(\dot{\gamma},t)$ for 30 wt % lyotropic solution of PSHQ4−7CNCOOH in *o*-dichlorobenzene at $\dot{\gamma} = 0.08\ s^{-1}$ and three different temperatures (°C): 25, 23, and 15.

Figure 8 describes time evolution of $N_1^+(\dot{\gamma},t)$ and $\sigma^+(\dot{\gamma},t)$ at $\dot{\gamma} = 0.08\ s^{-1}$ for 30 wt % lyotropic solution of PSHQ4−7CNCOOH at 25, 23, and 15 °C. Note that the T_{cl} of the solution is 28 °C (see Table 1). It can be seen from Figure 8 that at 25 °C $N_1^+(\dot{\gamma},t)$ goes through a large overshoot followed by a small overshoot and then reaches steady state. But the steady-state value (N_1) is positive, which is quite different from that observed for the 25 wt % lyotropic solution. Notice that the highest measurement temperature for both solutions is 3 °C below the respective T_{cl}s. Again, the magnitude of N_1 for the 30 wt % lyotropic solution increases as the measurement temperature is decreased from 25 to 15 °C. The time evolution of $\sigma^+(\dot{\gamma},t)$ for the 30 wt % lyotropic solution is similar to that of $N_1^+(\dot{\gamma},t)$, except that there is only a single overshoot in $\sigma^+(\dot{\gamma},t)$.

Figure 9 describes (a) the dependence of $N_1^+(\dot{\gamma},t)$ on strain ($\dot{\gamma}t$) and (b) the dependence of $\sigma^+(\dot{\gamma},t)$ on $\dot{\gamma}t$ for 25 wt % lyotropic solution of PSHQ4−7CNCOOH at 12 °C for five different shear rates: 0.02, 0.06, 0.08, 0.10, and 0.15 s^{-1}. The following observations are worth noting in Figure 9a. (i) Upon startup of shear flow, the peak value of $N_1^+(\dot{\gamma},t)$ increases as $\dot{\gamma}$ is increased from 0.02 to 0.15 s^{-1}, (ii) $N_1^+(\dot{\gamma},t)$ at $\dot{\gamma} = 0.02\ s^{-1}$ steadily increases until reaching steady state (○), (iii) $N_1^+(\dot{\gamma},t)$ at $\dot{\gamma} = 0.06\ s^{-1}$ shows a negative value at steady state (△), (iv) $N_1^+(\dot{\gamma},t)$ at $\dot{\gamma} = 0.08\ s^{-1}$ shows a pronounced negative value at steady state (□), and (v) negative values of N_1 become smaller as $\dot{\gamma}$ is increased further to 0.15 s^{-1}. On the other hand, we observe from Figure 9b that values of steady-state shear stress (σ) are positive at all shear rates tested, the magnitude of which increases with increasing $\dot{\gamma}t$.

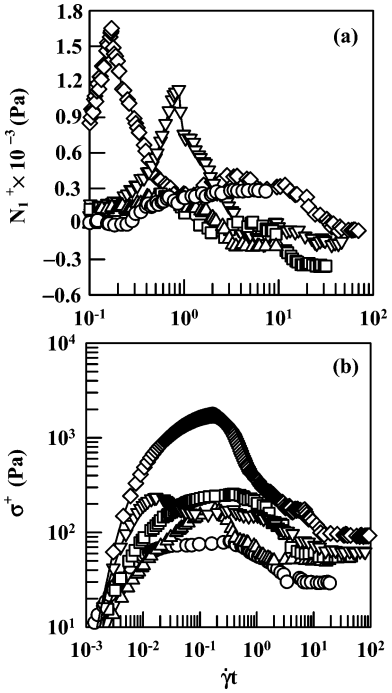

Figure 9. Plots, upon start-up of shear, of (a) first normal stress difference $N_1^+(\dot{\gamma},t)$ vs shear strain $\dot{\gamma}t$ and (b) shear stress $\sigma^+(\dot{\gamma},t)$ vs shear strain $\dot{\gamma}t$ at 12 °C for 25 wt % lyotropic solution of PSHQ4−7CNCOOH in *o*-dichlorobenzene at five different shear rates $\dot{\gamma}$ (s^{-1}): (○) 0.02, (△) 0.06, (□) 0.08, (▽) 0.10, and (◇) 0.15.

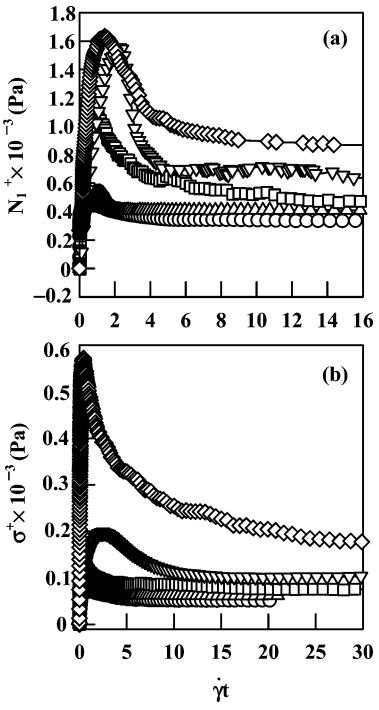

Figure 10. Plots, upon start-up of shear, of (a) first normal stress difference $N_1^+(\dot{\gamma},t)$ vs shear strain $\dot{\gamma}t$ and (b) shear stress $\sigma^+(\dot{\gamma},t)$ vs shear strain $\dot{\gamma}t$ at 23 °C for 30 wt % lyotropic solution of PSHQ4−7CNCOOH in *o*-dichlorobenzene at five different shear rates $\dot{\gamma}$ (s^{-1}): (○) 0.04, (△) 0.06, (□) 0.08, (▽) 0.12, and (◇) 0.20.

Figure 10 describes (a) the dependence of $N_1^+(\dot{\gamma},t)$ on $\dot{\gamma}t$ and (b) the dependence of $\sigma^+(\dot{\gamma},t)$ on $\dot{\gamma}t$ for 30 wt % lyotropic solution of PSHQ4−7CNCOOH at 23 °C for five different shear rates: 0.02, 0.06, 0.08, 0.10, and 0.15 s^{-1}. For all shear rates investigated, $N_1^+(\dot{\gamma},t)$ shows a single overshoot followed by decay toward steady state. In other words, no negative values

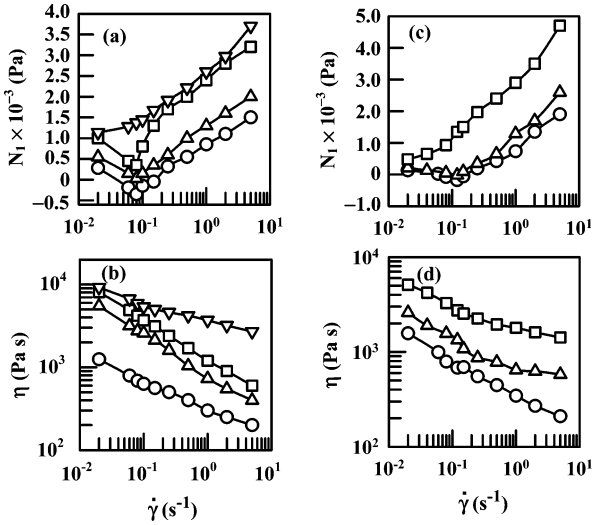

Figure 11. The left-side panel describes (a) first normal stress difference N_1 vs shear rate $\dot{\gamma}$ and (b) viscosity η vs shear rate $\dot{\gamma}$ in steady-state shear flow of 25 wt % lyotropic solution of PSHQ4−7CNCOOH in *o*-dichlorobenzene at four different temperatures (°C): (○) 12, (△) 8, (□) 5, and (▽) 0. The right-side panel describes (c) N_1 vs $\dot{\gamma}$ and (d) η vs $\dot{\gamma}$ in steady-state shear flow of 27 wt % lyotropic solution of PSHQ4−7CNCOOH in *o*-dichlorobenzene at three different temperatures (°C): (○) 17, (△) 13, and (□) 10.

of N_1 are observed at all five different shear rates employed. The time evolution of $\sigma^+(\dot{\gamma},t)$ for the same lyotropic solution follows a very similar pattern as that of $N_1^+(\dot{\gamma},t)$.

(c) Steady-State Shear Properties of Lyotropic Solutions of PSHQ4−7CNCOOH. Figure 11 describes (a) the shear-rate dependence of first normal stress difference (N_1) and (b) the shear-rate dependence of viscosity (η) in steady-state shear flow for 25 wt % lyotropic solution (the left-side panel) at four temperatures (12, 8, 5, and 0 °C) and (c) the shear-rate dependence of N_1 and (d) the shear-rate dependence of η in steady-state shear flow for 27 wt % lyotropic solution (the right-side panel) at three different temperatures (17, 13, and 10 °C). It can be seen in Figure 11a (in the upper left side) that at 12 °C the N_1 for 25 wt % lyotropic solution is positive at $\dot{\gamma} = 0.02$ s^{-1}, becomes negative at $\dot{\gamma} = 0.06$, 0.08, and 0.12 s^{-1}, and then becomes positive again at $\dot{\gamma} = 0.25$ s^{-1} and higher shear rates. That is, N_1 goes through negative values at the intermediate shear rates, this observation being very similar to that first made in the seminal studies[2−4] by Kiss and Porter, who employed lyotropic solutions of PBLG in *m*-cresol, and later by other investigators,[16−18,21] who employed lyotropic solutions of HPC in *m*-cresol or water. Notice in Figure 11a that values of N_1 are shifted upward, while still exhibiting a minimum, as the temperature is decreased from 12 to 8 and to 5 °C, but the value of N_1 at 5 °C no longer has a negative sign at $\dot{\gamma} = 0.08$ s^{-1} at which a minimum in N_1 is still observed. Interestingly enough, however, not only a minimum in N_1 but also the negative sign of N_1 disappear completely over the entire range of $\dot{\gamma}$ investigated when the temperature is decreased further down to 0 °C! Similar shear-rate dependence of N_1 is observed in Figure 11c (in the upper right side) for 27 wt % lyotropic solution, but the magnitude of the minimum in N_1 is much smaller than that for 25 wt % lyotropic solution (see Figure 11a), and once again, not only a minimum in N_1 but also the negative sign of N_1 disappear completely over the entire range of $\dot{\gamma}$ investigated when the temperature is decreased further down to 10 °C. On the other hand, as intuitively expected, values of η increase steadily as the temperature is decreased in both 25 and 27 wt % lyotropic solutions, and only shear-thinning behavior is

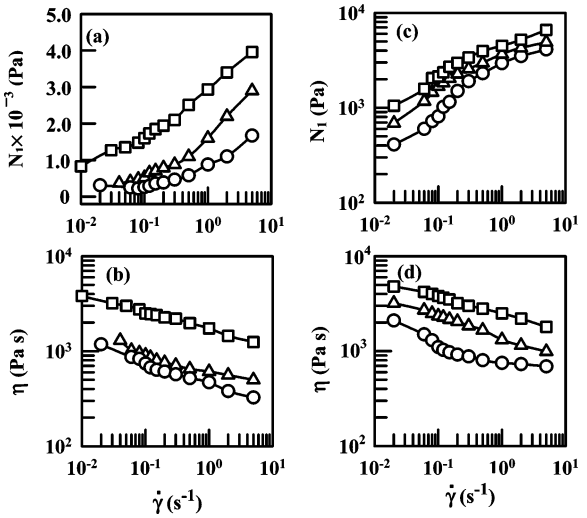

Figure 12. The left-side panel describes (a) first normal stress difference N_1 vs shear rate $\dot{\gamma}$ and (b) viscosity η vs shear rate $\dot{\gamma}$ in steady-state shear flow of 30 wt % lyotropic solution of PSHQ4−7CNCOOH in *o*-dichlorobenzene at three different temperatures (°C): (○) 25, (△) 23, and (□) 15. The right-side panel describes (c) N_1 vs $\dot{\gamma}$ and (d) η vs $\dot{\gamma}$ in steady-state shear flow of 40 wt % lyotropic solution of PSHQ4−7CNCOOH in *o*-dichlorobenzene at three different temperatures (°C): (○) 40, (△) 30, (□) 20.

observed over the entire range of $\dot{\gamma}$ investigated (i.e., only region I exists) (see Figure 11b,d).

Figure 12 describes (a) the shear-rate dependence of N_1 and (b) the shear-rate dependence of η in steady-state shear flow for 30 wt % lyotropic solution (the left-side panel) at three temperatures (25, 23, and 15 °C) and (c) the shear-rate dependence of N_1 and (d) the shear-rate dependence of η in steady-state shear flow for 40 wt % lyotropic solution (the right-side panel) at three different temperatures (40, 30, and 20 °C). It can be seen in Figure 12a that not only are the values of N_1 positive, but also no minimum in N_1 is observed over the entire range of shear rates investigated at all three temperatures. Notice further that values of N_1 increase with increasing $\dot{\gamma}$ and with decreasing temperature, as observed in main-chain TLCPs[31−36,38−40] and side-chain TLCPs[52,55,56] as well as in PSHQ4−7CNCOOH thermotrope (see Figure 2). That is, N_1 for 30 wt % lyotropic solution of PSHQ4−7CNCOOH is positive over the entire range of shear rates and temperatures investigated. The same observation can be made from Figure 12c for 40 wt % lyotropic solution of PSHQ4−7CNCOOH, except that the magnitude of N_1 for the 40 wt % lyotropic solution is much greater than that for the 30 wt % lyotropic solution at the same distance from the respective T_{cl}s. For example, compare the shear-rate dependence of N_1 at 25 °C in Figure 12a for the 30 wt % lyotropic solution with that at 40 °C in Figure 12c for the 40 wt % lyotropic solution, where the measurement temperatures are 3 °C below the respective T_{cl}s (see Table 1). Again, the shear-rate dependence of η given in Figure 12b for the 30 wt % lyotropic solution and in Figure 12d for the 40 wt % lyotropic solution is as expected in that values of η decrease with increasing $\dot{\gamma}$ and with decreasing temperature. Further, the magnitude of η for the 40 wt % lyotropic solution is greater than that for the 30 wt % lyotropic solution at the same distance from the respective T_{cl}s. We have taken rheological measurements for other lyotropic solutions having different concentrations. For the sake of completeness, such results for 22, 50, and 60 wt % lyotropic solutions are given in the Supporting Information. It should be mentioned that during our investigation the rheological measurements were repeated 4−5 times for each concentration, shear rate, and temperature employed, and we have found them to be absolutely reproducible. The uncertainties associated with our experimental results are too small to be put in Figures 11 and 12.

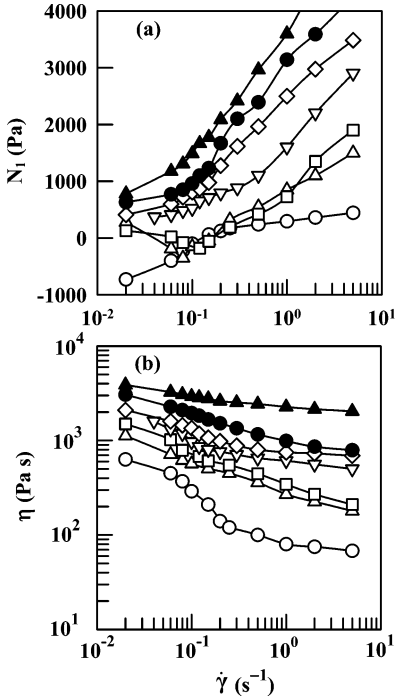

Figure 13. Plots of (a) first normal stress difference N_1 vs shear rate $\dot{\gamma}$ and (b) viscosity η vs shear rate $\dot{\gamma}$ in steady-state shear flow of lyotropic solutions of PSHQ4−7CNCOOH in *o*-dichlorobenzene having various concentrations (wt %): (○) 22, (△) 25, (□) 27, (▽) 30, (◇) 40, (●) 50, and (▲) 60 at 3 °C below the respective clearing temperatures.

Figure 13 describes the effect of concentration on (a) the shear-rate dependence of N_1 and (b) the shear-rate dependence of η in steady-state shear flow for seven different concentrations of lyotropic solutions of PSHQ4−7CNCOOH at 3 °C below the respective T_{cl}s (see Table 1). It is seen in Figure 13 that a critical concentration exists, below which negative values of N_1 are observed at intermediate shear rates and N_1 is positive with increasing concentration above the critical value. Needless to state, such a critical concentration would vary with the chemical structure of LCP that exhibits lyotropic characteristics. Over the entire range of concentrations investigated, the viscosities of the lyotropic solutions of PSHQ4−7CNCOOH show only shear-thinning behavior (only region I exists).

Figure 14 describes the concentration dependence of N_1 and η for the seven lyotropic solutions of PSHQ4−7CNCOOH at 3 °C below the respective T_{cl}s. The shape of the plots given in Figure 14 would depend strongly on temperature. Figure 14 was prepared to illustrate that the sign of N_1 for lyotropic solutions depends on solution concentration at a fixed temperature. Earlier, Baek et al.[18] made similar observations for lyotropic solutions of HPC, although not explicitly as shown in Figure 14.

(d) Reversal Flow of Lyotropic Solutions of PSHQ4−7CNCOOH. We also conducted flow reversal experiments for lyotropic solutions of PSHQ4−7CNCOOH to observe whether shear stress and first normal stress difference scale with strain. Figure 15 gives plots of (a) normalized shear stress $\sigma^+(t,\dot{\gamma})/\sigma$ vs shear strain $\dot{\gamma}t$ and (b) normalized first normal stress difference $N_1^+(t,\dot{\gamma})/N_1$ vs $\dot{\gamma}t$, upon flow reversal, for 25 wt % PSHQ4−7CNCOOH in *o*-dichlorobenzene at 12 °C for three different shear rates: (○) 0.06, (△) 0.08, and (□) 0.15. In reference to Figure 9 note that N_1 is negative for $\dot{\gamma} = 0.06$,

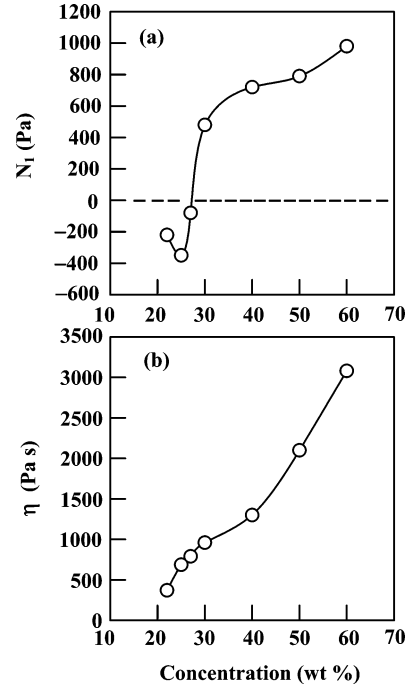

Figure 14. Plots of (a) first normal stress difference N_1 vs concentration and (b) viscosity η vs concentration in steady-state shear flow at $\dot{\gamma} = 0.08\ s^{-1}$ for seven different lyotropic solutions of PSHQ4−7CNCOOH in *o*-dichlorobenzene at 3 °C below the respective clearing temperatures.

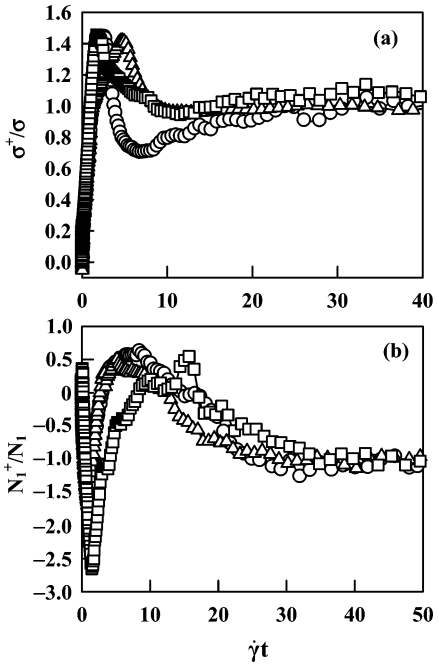

Figure 15. Plots of (a) normalized shear stress difference σ^+/σ vs shear stain $\dot{\gamma}t$ and (b) normalized first normal stress difference N_1^+/N_1 vs shear stain $\dot{\gamma}t$, upon flow reversal, for 25 wt % lyotropic solution of PSHQ4−7CNCOOH in *o*-dichlorobenzene at 12 °C for three different shear rates (s^{-1}): (○) 0.06, (△) 0.08, and (□) 0.15.

0.08, and 0.15 s^{-1}. In Figure 15 we observe that both shear stress and first normal stress difference do *not* scale with strain.

Only a few research groups have reported on strain scaling of shear stress for lyotropic solutions, after a reversal in flow direction. Moldenaers et al.[60] observed that the ratio $\sigma^+(t,\dot{\gamma})/\sigma$ scaled with $\dot{\gamma}t$ after the reversal in flow direction had occurred in a lyotropic solution of 12 wt % PBLG in *m*-cresol. Burghardt and Fuller,[61] who employed lyotropic solutions of PBG in *m*-cresol, made a similar observation. On the other hand, Hongladarom and Burghardt[12] did *not* observe strain scaling with the ratio $\sigma^+(t,\dot{\gamma})/\sigma$ for lyotropic solutions of HPC in water after the reversal in flow direction. The situation appears to be very complicated in that Walker et al.[13] observed strain scaling with the ratio $\sigma^+(t,\dot{\gamma})/\sigma$ for a lyotropic solution of 37 wt % PBLG in *m*-cresol, but not for a lyotropic solution of 40 wt % PBLG in *m*-cresol, after the reversal in flow direction. It is then fair to state that no general conclusion can be drawn on strain scaling for LCPs after the reversal in flow direction.

Very few papers have reported on strain scaling with $N_1^+(t,\dot{\gamma})$ for lyotropic LCPs after reversal in flow direction. Chow et al.[62] reported variations of $N_1^+(t,\dot{\gamma})$with $\dot{\gamma}t$ for lyotropic solutions of poly(*p*-phenylenebenzobisthiazole) (PBZT) after reversal in flow direction, indicating that, for this system, $N_1^+(t,\dot{\gamma})$ does not follow strain scaling after flow reversal. In this regard, the experimental results given in Figure 15 for the 25 wt % lyotropic solution of PSHQ4−7CNCOOH are in general agreement with the experimental results of Chow et al.

4. Discussion

Since the seminal experimental study of Kiss and Porter,[2] who in 1978 reported on negative values of N_1 in steady-state shear flow of PBLG in *m*-cresol over a certain range of shear rates, several theoretical attempts have been made to explain the origin of such an unusual experimental observation. Currie[63] appears to be the first who in 1981 considered steady-state shear flow of low-molecular-weight nematics (liquid crystals) using the Leslie−Ericksen theory[64,65] and concluded that N_1 can be positive or negative or change from negative to positive with increasing shear stress depending on the so-called boundary orientation. Further, he related the sign of N_1 to the Leslie angle. However, the sign change in N_1 from positive to negative and then back to positive (with increasing shear stress), which had been observed for lyotropic PBLG solutions by Kiss and Porter,[2] was not predicted for liquid crystals. Subsequently, in 1984 Carlsson[66] solved numerically the equations governing the steady-state shear flow of nematic liquid crystals using the Leslie−Ericksen theory and calculated the director and velocity profiles under the assumption that the director remained in the plane of shear. His analysis predicted that above a certain critical shear rate the director tumbles[67] depending upon the sign of the Leslie coefficients, α_2 and α_3. Specifically, for the situations where $\alpha_2\alpha_3 < 0$ with $\alpha_3 > 0$ and $\alpha_2 < 0$ is held, the flow alignment in the plane of shear does not occur; i.e., the director tumbles. Independently, in 1984 Kuzuu and Doi[68] considered simple shear flow of concentrated solutions of rodlike polymers based on the Doi molecular theory[69] and then obtained via numerical calculations, with some simplifying assumptions together with the Onsager potential,[70] a relationship between a tumbling parameter λ and concentration *C*. According to Kuzuu and Doi (see Figure 1 in ref 68), the tumbling parameter λ describes the stability of simple shear flow; namely, stable shear flow exists, and thus the director makes constant angles when $\lambda > 1$, and no stable shear flow is possible and thus the director tumbles when $\lambda < 1$ above a critical concentration C^* of lyotropic solutions of rodlike polymers.

Two significant papers were published in 1989 by Marrucci and Maffettone[57] and in 1990 by Larson,[58] explaining the origin of negative N_1 in shear flow of lyotropic solutions of rodlike polymers. Specifically, using the Maier−Saupe potential,[71] Marrucci and Maffettone conducted a two-dimensional analysis of shear flow of the nematic monodomains of lyotropic solutions of rodlike polymers and obtained analytic expressions relating the sign of N_1 to director tumbling. They concluded that the

occurrence of a negative N_1 is associated with a flow transition between director tumbling and flow-aligning behavior. On the other hand, Larson[58] carried out a three-dimensional analysis of shear flow of the nematic monodomains of lyotropic solutions of rodlike polymers, for which he used the Doi theory[69] together with the Onsager potential[70] and solved numerically the system equations by expansion in spherical harmonic functions. He predicted the circumstances under which the director tumbles in shear flow and concluded that negative N_1 occurs in the "wagging" regime representing the transition from the tumbling to the nontumbling flow (flow-aligning) regime (see Figure 11 in ref 58). The three-dimensional Larson analysis supports the two-dimensional Marrucci−Maffettone analysis in that negative N_1 is associated with a flow transition between director tumbling and flow-aligning behavior.

It is appropriate to discuss at this juncture the relevance, if any, of the theoretical investigations cited above to the experimental results summarized in this paper. There are three issues to be addressed here. (i) The PSHQ4−7CNCOOH employed in our experimental study has flexible spacers in both the main chain and side chain and thus it is not a rodlike polymer, while the Marrucci−Maffettone and Larson analyses dealt with lyotropic solutions of rodlike polymers. (ii) The PSHQ4−7CNCOOH employed in our experimental study has nematic polydomains with defects (see Figure 6), while the Marrucci−Maffettone and Larson analyses dealt with the nematic monodomains of lyotropic solutions. (iii) An appropriate expression(s) for the excluded-volume potential for the PSHQ4−7CNCOOH employed in our experimental study is not known, while the Marrucci−Maffettone analysis is based on the Maier−Saupe potential that is believed to be suitable low-molecular-weight liquid crystals, and the Larson analysis is based on the Onsager potential that is believed to be suitable for very dilute concentrations. (iv) In the formulation of the Marrucci−Maffettone and Larson analyses the elasticity of the defect texture was not included. One may then argue that an interpretation of our experimental results presented here using the Marrucci−Maffettone and Larson analyses may not be warranted.

In our investigation we have observed a sign change in N_1 (from positive to negative and then back to positive with increasing shear rate) over a narrow range of shear rates for only 22, 25, and 27 wt % lyotropic solutions of PSHQ4−7CNCOOH and positive values of N_1 for higher concentrations. This does not necessarily mean that a sign change in N_1 may not occur outside the shear rate range over which normal stress measurements were taken in the present study. Since we did not conduct experiments to determine whether the director tumbled in the shear rate range over which a sign change in N_1 was observed, we are not in a position to state whether the experimentally observed negative N_1 is associated with a flow transition between director tumbling and flow-aligning behavior. Nevertheless, it is fair to state that our experimental results of sign change in N_1 in steady-state shear flow of some (22, 25, and 27 wt %) lyotropic solutions of PSHQ4−7CNCOOH are in line with the theoretical predictions by the Marrucci−Maffettone and Larson analyses.

Whether an LCP is of tumbling type or flow-aligning can be investigated using rheooptical methods. Indeed, some investigators[61,72] reported on director tumbling in some lyotropic LCPs. On the other hand, the experimental studies based on in-situ X-ray scattering[40,73] and in-situ conoscopy[74] indicate that thermotropic LCPs are flow-aligning. Numerous investigators have employed various rheooptical methods (e.g., X-ray, birefringence, dichroism) to investigate molecular alignment and/or shear orientation behavior of lyotropic LCPs[5,11,12,19,60,75] and thermotropic LCPs.[42,76] In the future we will conduct a rheooptical investigation of lyotropic solutions of PSHQ4−7CNCOOH in order to determine whether some of the lyotropic solutions that have exhibited negative N_1 in the present study are of the tumbling type.

A rigorous interpretation of our experimental results with respect to the variations in temperature and concentration of the lyotropic solutions of PSHQ4−7CNCOOH employed in this study is very complex. According to the Larson theory,[58] which incorporates the Doi equation[69] although it is based on untextured rodlike LCPs as pointed out above, transitions between tumbling, wagging, and flow aligning regimes (and associated normal stress sign changes) occur at critical values of the Deborah number. Thus, changes in the molecular relaxation time with temperature or concentration could lead to dramatic changes in the Deborah number even when shear rate is held constant. Referring to Figure 11, for example, changes in temperature mean that the range of Deborah numbers is different for experiments at each temperature. Experiments at lower temperatures will actually be at higher Deborah numbers than those at higher temperatures. Since increasing Deborah number leads to changes from negative to positive N_1 in lyotropic solutions, this might contribute to the disappearance of the regime of negative N_1. Likewise, an increase in concentration will increase the molecular relaxation time and thus Deborah number even when shear rate and temperature are held constant. This then will lead to changes from negative to positive N_1 in lyotropic solutions, consequently contributing to the disappearance of the regime of negative N_1.

5. Concluding Remarks

In this paper we have presented the transient shear flow, steady-state shear flow, oscillatory shear flow, and time evolution of dynamic moduli upon cessation of shear flow of a combined main-chain/side-chain LCP, PSHQ4−7CNCOOH, in the thermotropic state. Only positive values of first normal stress difference (N_1) in steady-state shear flow were observed over the entire range of shear rates and temperatures investigated. For comparison, we also investigated the rheological behavior of a main-chain LCP, PSHQ4, which has exactly the same chemical structure as the main-chain backbone of PSHQ4−7CNCOOH. We found that at temperatures below the respective clearing temperatures of the two LCPs the frequency dependence of complex viscosity $|\eta^*|$ looks somewhat similar in both PSHQ4−7CNCOOH and PSHQ4, although PSHQ4−7CNCOOH shows shear-thinning behavior over the entire range of angular frequencies investigated. However, at angular frequencies less than 1 rad/s, the $|\eta^*|$ of PSHQ4 follows Newtonian behavior, while the $|\eta^*|$ of PSHQ4−7CNCOOH does not. Upon cessation of shear flow, the dynamic storage modulus G' of PSHQ4−7CNCOOH initially increases very fast and then levels off, reaching a constant value after ca. 50 min at 150 °C, after ca. 200 min at 140 °C, and after ca. 350 min at 130 °C. On the other hand, upon cessation of shear flow, the dynamic storage modulus G' of PSHQ4 does not attain a constant value even after 750 min upon cessation of shear flow. Since an increase in G' upon cessation of shear flow may be viewed as signifying a recovery of the deformed domain structure (i.e., structural reorganization) after shear flow stops, we conclude that upon cessation of shear flow a faster structural reorganization takes place in PSHQ4−7CNCOOH than in PSHQ4.

In this paper we have also presented the transient and steady-state shear flow behaviors of PSHQ4−7CNCOOH in the

lyotropic state, placing emphasis on the effects of concentration and temperature. Solutions of various concentrations (22−70 wt %) of PSHQ4−7CNCOOH dissolved in *o*-dichlorobenzene were prepared for rheological measurements. We have observed negative values of steady-state N_1 at intermediate shear rates for the lyotropic solutions of PSHQ4−7CNCOOH having concentrations of 22, 25, and 27 wt %, but only positive values of N_1 for higher concentrations over the entire range of shear rates investigated. We hasten to point out that the lack of a measurable range of negative N_1 does not preclude the possibility that N_1 is negative outside the experimental shear-rate range. Interestingly, we found that negative values of N_1 became positive as the measurement temperature decreased below a certain critical value. Thus, the sign change in N_1 depends on both the concentration and temperature of the lyotropic solutions of PSHQ4−7CNCOOH at a fixed shear rate. Also, flow reversal of lyotropic solutions of PSHQ4−7CNCOOH was investigated. We found that both shear stress and first normal stress difference do not follow strain scaling after flow reversal.

Regarding the sign change in steady-state N_1 for the lyotropic solutions of PSHQ4−7CNCOOH, the experimental observations made in this study are in consonance with the predictions of the Marrucci−Maffettone and Larson analyses,[57,58] although the analyses are based on defect-free rodlike monodomain LCPs, while PSHQ4−7CNCOOH is a semiflexible polydomian LCP. Since the present study dealt only with mechanical rheological measurements, we are not in a position to state whether PSHQ4−7CNCOOH is unequivocally of the tumbling type. In the near future we intend to conduct a rheooptical investigation of the lyotropic solutions of PSHQ4−7CNCOOH in order to determine whether the lyotropic solutions that have exhibited negative N_1 at intermediate shear rates in this study are of the tumbling type.

Acknowledgment. This study was supported in part by the Petroleum Research Funds (#PRF35694-AC7) of the American Chemical Society.

Supporting Information Available: Some rheological data for PSHQ4 and steady-state shear flow properties of additional lyotropic solutions of PSHQ4−7CNCOOH. This material is available free of charge via the Internet at http://pubs.acs.org.

Noted Added after ASAP Publication. This article was published ASAP on November 23, 2005. Changes have been made to refs 59 and 68. The correct version was posted on November 30, 2005.

References and Notes

(1) Hermans, J. *J. Colloid Sci.* **1962**, *17*, 638.
(2) Kiss, G.; Porter, R. S. *J. Polym. Sci., Polym. Symp.* **1978**, *65*, 193.
(3) Kiss, G.; Porter, R. S. *J. Polym. Sci., Polym. Phys. Ed.* **1980**, *18*, 361.
(4) Kiss, G.; Porter, R. S. *Mol. Cryst. Liq. Cryst.* **1980**, *60*, 267.
(5) Asada, T.; Muramatsu, H.; Watanabe, R.; Onogi, S. *Macromolecules* **1980**, *13*, 867.
(6) Moldenaers, P.; Mewis, J. *J. Rheol.* **1986**, *30*, 567.
(7) Mewis, J.; Moldenaers, P. *Mol. Cryst. Liq. Cryst.* **1987**, *153*, 291.
(8) Mead. D. W.; Larson, R. G. *Macromolecules* **1990**, *23*, 2524.
(9) Magda, J. J.; Baek, S. G.; De Vries, K. L.; Larson, R. G. *Macromolecules* **1991**, *24*, 4460.
(10) Baek, S. G.; Magda, J. J.; Larson, R. G. *J. Rheol.* **1993**, *37*, 1201.
(11) Hongladarom, K.; Burghardt, W. R.; Baek, S. G.; Cementwala, S.; Magda, J. J. *Macromolecules* **1993**, *26*, 772.
(12) Hongladarom, K.; Burghardt, W. R. *Macromolecules* **1993**, *26*, 785.
(13) Walker, L. M.; Wagner, N. J.; Larson, R. G.; Mirau, P. A.; Moldenaers, P. *J. Rheol.* **1995**, *39*, 925.
(14) Walker, L. M.; Mortier, M.; Moldenaers, P. *J. Rheol.* **1996**, *40*, 967.
(15) Navard, P.; Haudin, J. M. *J. Polym. Sci., Polym. Phys. Ed.* **1986**, *24*, 189.
(16) Grizzuti, N.; Cavella, S.; Cicarelli, P. *J. Rheol.* **1990**, *34*, 1293.
(17) Baek, S. G.; Magda, J. J.; Cementwala, S. *J. Rheol.* **1993**, *37*, 935.
(18) Baek, S. G.: Magda, J. J.; Larson, R. G.: Hudson, S. D. *J. Rheol.* **1994**, *38*, 1473.
(19) Hongladarom, K.; Secakusuma, V.; Burghardt, W. R. *J. Rheol.* **1994**, *38*, 1505.
(20) Hongladarom, K.; Ugaz, V. M.; Cinader, D. K.; Burghardt, W. R.; Quintana, J. P.; Hsiao, B. D.; Dadmun, M. D.; Hamilton, W. A.; Butler, P. D. *Macromolecules* **1996**, *29*, 5346.
(21) Huang, C. M.; Magda, J. J.; Larson, R. G. *J. Rheol.* **1999**, *43*, 31.
(22) Papkov, S. P.; Kulichikhin, B. G.; Kalmykovam, V. D.; Malkin, A. Ya. *J. Polym. Sci., Polym. Phys. Ed.* **1974**, *12*, 1753.
(23) Valenti, B.; Ciferri, A. *J. Polym. Sci., Polym. Lett. Ed.* **1978**, *16*, 657.
(24) Helminiak, T. E.; Berry, G. C. *J. Polym. Sci., Polym. Symp.* **1978**, *65*, 107.
(25) Wong, C. P.; Ohnuma, H.; Berry, G. C. *J. Polym. Sci., Polym. Symp.* **1978**, *65*, 173.
(26) Chu, G.; Venkatraman, S.; Berry, G. C.; Einaga, Y. *Macromolecules* **1981**, *14*, 939.
(27) Einaga, Y.; Berry, G. C.; Chu, S. G. *Polym. J.* **1985**, *17*, 239.
(28) Wissbrun, K. F.; Griffin, A. C. *J. Polym. Sci., Polym. Phys. Ed.* **1982**, *20*, 1835.
(29) Wunder, S. L.; Ramachandran, S.; Cochanour, C. R.; Weinberg, M. *Macromolecules* **1986**, *19*, 1696.
(30) Irwin, R. S.; Sweeny, W.; Gardner, K. H.; Gochanour, C. R.; Weinberg, M. *Macromolecules* **1989**, *22*, 1065.
(31) Driscoll, P.; Masuda, T.; Fujiwara, K. *Macromolecules* **1991**, *24*, 1567.
(32) Cocchini, F.; Nobile, M. R.; Acierno, D. *J. Rheol.* **1991**, *35*, 1171.
(33) Kim, S. S.; Han, C. D. *J. Rheol.* **1993**, *37*, 847.
(34) Kim, S. S.; Han, C. D. *Macromolecules* **1993**, *26*, 6633.
(35) Kim, S. S.; Han, C. D. *J. Polym. Sci., Part B: Polym. Phys.* **1994**, *32*, 371.
(36) Han, C. D.; Chang, S.; Kim, S. S. *Mol. Cryst. Liq. Cryst.* **1994**, *254*, 335.
(37) Gilmore, J. R.; Colby, R. H.; Hall, E.; Ober, C. K. *J. Rheol.* **1994**, *38*, 1623.
(38) Chang, S.; Han, C. D. *Macromolecules* **1997**, *30*, 1656.
(39) Chang, S.; Han, C. D. *Macromolecules* **1997**, *30*, 2021.
(40) Zhou, W. J.; Kornfield, J. A.; Ugaz, V. M.; Burghardt, W. R.; Link, D. R.; Clark, N. A. *Macromolecules* **1999**, *32*, 5581.
(41) Kim, D.-O.; Han, C. D. *Macromolecules* **2000**, *33*, 3349.
(42) Mather, P. T.; Jeon, H. G.; Han, C. D.; Chang, S. *Macromolecules* **2000**, *33*, 7594.
(43) Zentel, R.; Wu, J. *Makromol. Chem.* **1986**, *187*, 1727.
(44) Fabre, P.; Veyssie, M. *Mol. Cryst. Liq. Cryst. Lett.* **1987**, *4*, 99.
(45) Colby, R. H.; Gillmor, J. R.; Galli, G.; Laus, M.; Ober, C. K.; Hall, E. *Liq. Cryst.* **1993**, *13*, 233.
(46) Kannan, R. M.; Kornfield, J. A. *Macromolecules* **1993**, *26*, 2050.
(47) Kannan, R. M.; Rubin, S. F.; Kornfield, J. A.; Boeffel, C. *J. Rheol.* **1994**, *38*, 1609.
(48) Rubin, S. F.; Kannan, R. M.; Kornfield, J. A.; Boeffel, C. *Macromolecules* **1995**, *28*, 3521.
(49) Colby, R. H.; Ober, C. L.; Gilmor, J. R.; Connelly, R. W.; Duong, T.; Galli, G.; Laus, M. *Rheol. Acta* **1997**, *36*, 498.
(50) Berghausen, J.; Fuchs, J.; Richtering, W. *Macromolecules* **1997**, *30*, 7574.
(51) Quijada-Garrido, I.; Siebert, H.; Friedrich, C.; Schmidt, C. *Rheol. Acta* **1999**, *38*, 3495.
(52) Quijada-Garrido, I.; Siebert, H.; Friedrich, C.; Schmidt, C. *Macromolecules* **2000**, *33*, 3844.
(53) Wewerka, A.; Floudas, G.; Pakula, T.; Stelzer, F. *Macromolecules* **2001**, *34*, 8129.
(54) Wewerka, A.; Viertler, K.; Vlassopoulos, D.; Stelzer, F. *Rheol. Acta* **2001**, *40*, 416.
(55) Lee, K. M.; Han, C. D. *Macromolecules* **2002**, *35*, 6263.
(56) Lee, K. M.; Han, C. D. *Macromolecules* **2003**, *36*, 8796.
(57) Marrucci, G.; Maffettone, P. L. *Macromolecules* **1989**, *22*, 4076.
(58) Larson, R. G. *Macromolecules* **1990**, *23*, 3983.
(59) Zhou, M.; Han, C. D. *Macromolecules* **2005**, *38*, 9602.
(60) Moldenaers, P.; Fuller, G.; Mewis, J. *Macromolecules* **1989**, *22*, 2**,** 960.
(61) Burghardt, W. R.; Fuller, G. G. *Macromolecules* **1991**, *24*, 2546.
(62) Chow, A.; Hamlin, R. D.; Ylitalo, C. M. *Macromolecules* **1992**, *25*, 7135.
(63) Currie, P. K. *Mol. Cryst. Liq. Cryst.* **1981**, *73*, 1.
(64) Ericksen, J. L. *Arch. Ration. Mech. Anal.* **1960**, *4*, 231.
(65) Leslie, F. M. *Arch. Ration. Mech. Anal.* **1968**, *28*, 265.
(66) Carlsson, T. *Mol. Cryst. Liq. Cryst.* **1984**, *104*, 307.
(67) The director, the direction of average molecular orientation, will rotate indefinitely if the sign of α_3 is positive, and this phenomenon is referred to as director tumbling. Tumbling occurs when the director assumes no preferred angle with respect to the flow direction but

constantly rotates around the vorticity axis until Frank distortional stresses bring this rotation to a halt.
(68) Kuzuu, N.; Doi, M. *J. Phys. Soc. Jpn.* **1984**, *53*, 1031.
(69) Doi, M. *J. Polym. Sci., Polym. Phys. Ed.* **1981**, *19*, 229.
(70) Onsager, L. *Ann. N.Y. Acad. Sci.* **1949**, *51*, 627.
(71) (a) Maier, V. W.; Saupe, A. *Z. Naturforsch., A* **1958**, *13A*, 564. (b) *Z. Naturforsch., A* **1959**, *14A*, 882. (c) *Z. Naturforsch., A* **1960**, *15A*, 287.
(72) Srinivasarao, M.; Berry, G. C. *J. Rheol.* **1991**, *35*, 379.
(73) Ugaz, V. M.; Burghardt, W. R. *Macromolecules* **1998**, *31*, 8474.
(74) Zhou, W.-J.; Kornfield, J. A.; Burghardt, W. R. *Macromolecules* **2001**, *34*, 3654.
(75) Picken, S. J.; Aerts, J.; Visser, B.; Northolt, M. G. *Macromolecules* **1990**, *23*, 3849.
(76) Kim, D.-O.; Han, C. D.; Mather, P. T. *Macromolecules* **2000**, *33*, 7922.

MA050657A